Molecular Crystals and Liquid Crystals

ISSN: 1542-1406 (Print) 1563-5287 (Online) Journal homepage: http://www.tandfonline.com/loi/gmcl20

Asymmetric magnetoresistance in the graphite intercalation compounds with cobalt

V. Ya. Tkachuk, I. V. Ovsiyenko, L. Yu. Matzui, T. A. Len, Yu. I. Prylutskyy, O. A. Brusylovets, I. B. Berkutov, I. G. Mirzoiev & O. I. Prokopov

To cite this article: V. Ya. Tkachuk, I. V. Ovsiyenko, L. Yu. Matzui, T. A. Len, Yu. I. Prylutskyy, O. A. Brusylovets, I. B. Berkutov, I. G. Mirzoiev & O. I. Prokopov (2016) Asymmetric magnetoresistance in the graphite intercalation compounds with cobalt, Molecular Crystals and Liquid Crystals, 639:1, 137-150, DOI: 10.1080/15421406.2016.1255069

To link to this article: http://dx.doi.org/10.1080/15421406.2016.1255069

Published online: 14 Dec 2016.

MOLECULAR CRYSTALS AND LIQUID CRYSTALS
2016, VOL. 639, 137–150
http://dx.doi.org/10.1080/15421406.2016.1255069

Taylor & Francis
Taylor & Francis Group

Asymmetric magnetoresistance in the graphite intercalation compounds with cobalt

V. Ya. Tkachuk[a], I. V. Ovsiyenko[a], L. Yu. Matzui[a], T. A. Len[a], Yu. I. Prylutskyy[b], O. A. Brusylovets[c], I. B. Berkutov[d], I. G. Mirzoiev[d], and O. I. Prokopov[a]

Taras Shevchenko National University of Kyiv, Faculties of Physics[a], Biophysics[b], and Chemistry[c], Kyiv, Ukraine; [d]Verkin Institute for Low Temperature Physics and Engineering of the NAS of Ukraine, Kharkiv, Ukraine

ABSTRACT
The results of measurements of the magnetoresistance for graphite intercalation compounds with cobalt based on highly oriented pyrolytic graphite and fine crystalline pyrolytic graphite in the temperature range from 1.6 K to 293 K and in a magnetic field up to 16 T are presented. For the investigated intercalation compounds, the effect of asymmetry of the magnetoresistance relative to the magnetic field direction is revealed. It is shown that this effect can be satisfactorily explained within the Segal model of asymmetric magnetoresistance in thin films with large magnetic anisotropy.

KEYWORDS
graphite intercalation compound; asymmetric magnetoresistance; extraordinary Hall effect; cluster structure

Introduction

Due to the significant progress in the development of spintronics, the efforts of researchers are currently focused on the creation of magnetic nanostructures of different types, which have combined magnetic and nonmagnetic phases. In this view, the considerable attention is paid to the study of magnetic systems based on carbon nanostructures of different dimensions, which can be used as magnetic memory elements, magnetic sensors, molecular spintronic devices, etc.

A new wave of interest in those materials is caused by the appearance of some new theoretical calculations of the electronic structure and transport properties of the "graphene-metal" and "carbon nanotube-metal" systems [1–3]. The calculations conducted in [4, 5] showed that the interaction of magnetic atoms (Co, Fe) with carbon nanotubes (CNTs) and graphene could lead to the formation of semimetal nanosystems. The calculations for a graphene modified with magnetic metals [1, 4] indicate that the interaction between the metal atoms and carbon atoms leads to a gap in the electronic spectrum, which corresponds to spin-polarized states. It was shown in [5] that the encapsulation of Co and Fe in CNTs leads to a polarization of 90% of charge carriers. For Cr and V, this value can reach 100%. Similar results were obtained in [6–8] for some graphene-metal systems. Obviously, a carbon structure modification by magnetic metals, in particular, the introduction of magnetic metal particles in the inner cavity of a CNT and the deposition of magnetic metal particles on the CNT surface, the intercalation of magnetic metals atoms between layers of graphite, and a modification of

CONTACT I. V. Ovsiyenko ovsienko@mail.univ.kiev.ua

graphene with atoms of magnetic metals alter not only their electronic structure, but also lead to changes in magnetic properties of the modified carbon structure.

For partially oriented multiwall CNTs, the principal mechanism of magnetoresistance is the localization mechanism [9, 10], whereas the magnetoresistance of the same CNT filled in the inner cavity is determined by a combination of two mechanisms, namely, giant magnetoresistance and anisotropic magnetoresistance [11]. The similar magnetoresistance mechanisms were revealed for CNTs modified with cobalt and nickel [12]. Of a particular interest is the study of graphite intercalated with magnetic metals, in which the non-magnetic graphite layers alternate with layers of a magnetic metal [13, 14]. In these intercalation compounds, a number of new, not typical of graphite intercalation compounds (GICs) with nonmagnetic intercalates, properties appear [13, 15, 16]. In particular, in GICs with iron and cobalt, the extraordinary Hall effect is detected, which manifests itself in magnetic materials and is associated with a magnetic moment of the atoms of these materials. Another anomalous property, which is experimentally determined in the GICs with cobalt and nickel, is the magnetoresistance anisotropic (AMR) relative to the direction of a magnetic field.

It is known that the mechanisms of magnetoresistance in different materials are quite different, for example, the ordinary magnetoresistance in nonmagnetic metals and semiconductors, the anisotropic magnetoresistance in ferromagnetic materials, and the giant magnetoresistance in metallic multilayer structures. But, for all of them, the Onsager reversibility principle is true, i.e., $\Delta R_{xx}(B) = \Delta R_{xx}(-B)$. However, it was experimentally observed in some cases that this fundamental rule is violated [17, 18]. In spite of all attempts to explain the nature of this phenomenon, there is currently no general view of the mechanism of AMR formation. In [19], the origin of AMR in a doped quantum-dimensional structure in a magnetic field parallel to the heterostructure plane was associated with the simultaneous action on the charge carriers by the external electromagnetic fields and the internal field of space charges or the contact potential caused by the asymmetry of the quasimomentum spectrum of carriers. Another mechanism of AMR in multilayer Co-Pt films was proposed in [20, 21], according to which the formation in the material of domain walls perpendicular to the directions of the magnetic and electric fields leads to the abnormal Hall voltage having opposite polarities on opposite sides of domain walls. This abnormal Hall voltage is the cause for a distortion of the current. For ferromagnetic systems with a high degree of magnetic anisotropy, Segal et al. [22] proposed a model, in which the appearance of AMR is associated with a heterogeneous character of the magnetization along the specimens and the occurrence of the anomalous Hall effect in then. In presented paper, we will explain AMR in GICs based on the different types of graphites in terms of the Segal model.

Experimental and sample characterization

The GICs with cobalt were synthesized within a two-stage method with the usage of C_8K as a precursor [14]. According to the reaction $8C + K \rightarrow C_8K$, the intercalated compound with potassium was obtained at the first stage. At the second stage, the reduction of cobalt chloride (II) to cobalt metal with the subsequent substitution of potassium atoms by cobalt atoms in the interplanar spacing was performed. The reaction of reduction of cobalt chloride was running in a tetrahydrofurane (THF) medium according to the scheme: $2C_8K + CoCl_2$ (in THF solution) $\rightarrow C_{16}Co + 2KCl$. As a result, the GICs with cobalt were obtained. As a source material for the intercalation, two types of graphite with different structure perfections were used. These are highly oriented pyrolytic graphite (HOPG) (distance between layers $d_{002} = 0.335$ nm, crystallite size $L \sim 100$ nm) and fine crystalline pyrolytic graphite (FPG)

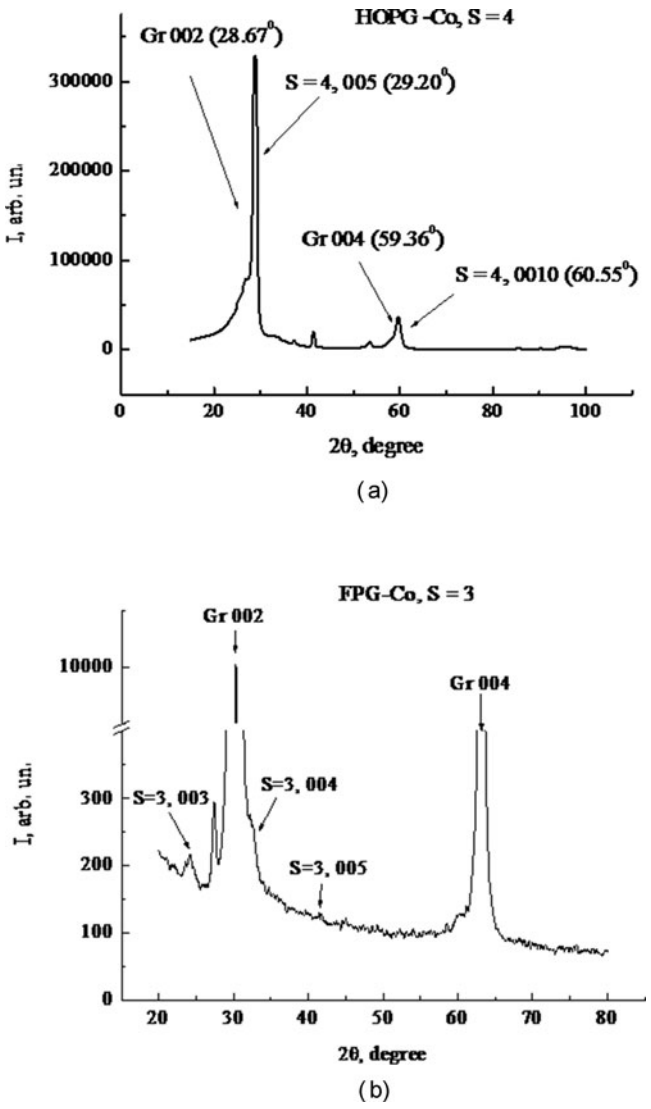

Figure 1. X-ray diffraction patterns for the GICs with cobalt based on HOPG (a) and FPG (b).

($d_{002} = 0.340$ nm, $L \sim 30$ nm). For both types of graphite, there is a significant anisotropy of the reduced crystalline structure. The structure and phase composition of the obtained GICs specimens were studied by a DRON-4-07 automated X-ray diffractometer. Figure 1 presents the fragments of the X-ray diffraction pattern for intercalated compounds based on HOPG (Fig. 1a) and on FPG (Fig. 1b).

As seen from Fig. 1, in addition to the graphite lines 002 and 004, the diffraction patterns contain also lines corresponding to the reflection from cobalt layers, which are placed between layers of graphite. The analysis of X-ray diffraction data shows that the obtained specimens are based on the HOPG compound of the fourth stage (specimen #1) and based on FPG compounds of the second (specimen #2) and third stages (specimen #3). The structure parameters (stage number S, identity parameter I_s, distance between two graphite layers containing the intercalate layer d_s) of the obtained GICs are given in Table 1.

A more detailed description of the structure of GICs is presented in [14].

Table 1. The structure parameters (stage number *S*, identity parameter I_s, distance between two graphite layers containing intercalate layer d_s) of obtained GICs.

#	GICs	*S*	I_s, nm	d_s,nm
1	HOPG-Co	4	1.645	0.64
2	FPG-Co	2	0.94	0.61
3	FPG-Co	3	1.278	0.61

The measurements of the resistance in a transverse magnetic field were carried out by standard four-probe method in the temperature interval from 1.6 K to 293 K and in magnetic fields up to 14 T. The measurement error does not exceed 0.05%. The magnetoresistance is calculated as $\frac{\Delta\rho}{\rho} = \frac{\rho(B)-\rho_0}{\rho_0}$, where ρ(B) is the resistivity in a magnetic field, ρ_0 is the resistivity without magnetic field.

Results and discussion

Figure 2 presents the field dependences of the magnetoresistance $\Delta\rho/\rho$(B) for sources for intercalation HOPG (Fig. 2a) and FPG (Fig. 2b) at 293 K and 77 K.

As is shown in Fig. 2a, the $\Delta\rho/\rho$(B) dependence on HOPG is typical of graphite with the structure of natural monocrystalline graphite. The magnetoresistance is symmetric relative to a magnetic field direction and is proportional to the squared magnetic field. As the temperature decreases, the magnetoresistance increases. For FPG, the magnetoresistance is also symmetric relative to the field and is positive at room temperature. But, as is seen in Fig. 2b, as the temperature decreases, the change of the magnetoresistance sign occurs, and, at 77 K, the magnetoresistance is negative. As is known, such temperature dependence of the magnetoresistance in FPG is explained by the manifestation of quantum effects of weak localization ant interaction of charge carriers [23].

Figure 3 presents the field dependences of the magnetoresistance $\Delta\rho/\rho$ (B) for intercalated compounds based on HOPG (Fig. 3a) and FPG (Fig. 3b, c) at several temperatures.

As is shown in the above figures, the cobalt intercalation into graphite results in significantly different dependences $\Delta\rho/\rho$(B) compared with the graphite source. For GICs based on FPG, the AMR is observed. For GICs based on HOPG, the difference between the values of magnetoresistance in the maximum magnetic field at opposite directions of field is ~7.8%. On the third stage, this difference at the temperature T = 4.2 K and the magnetic field B = 3.6 T is ~1.28%. On the second stage at the temperature T = 5 K and the same magnetic field, this difference is ~17.5%. Moreover, as is seen from Fig. 4, the character of the magnetoresistance field dependence for GICs based on FPG is changed. Unlike the FPG source, whose magnetoresistance is negative at temperatures below 77 K and the absolute value of the magnetoresistance increases with the magnetic field according to the square law, the magnetoresistance of GICs based on FPG is negative only in the certain range of a magnetic field. Furthermore, this interval depends on the measurement temperature and on the stage of compounds, i.e., the concentration of additional charge carriers in graphite planes. For example, on the second stage at T = 5 K, the magnetoresistance in the direction of the magnetic field is negative up to B = 15 T and is positive in the other field direction from B = 1 T. For the third stage, the transition from the negative to positive magnetoresistance at T = 5 K is observed in the magnetic field B = 2.3 T. As the temperature increases, the interval of magnetic fields, in which the magnetoresistance is negative, decreases. Note that, for all specimens of GICs

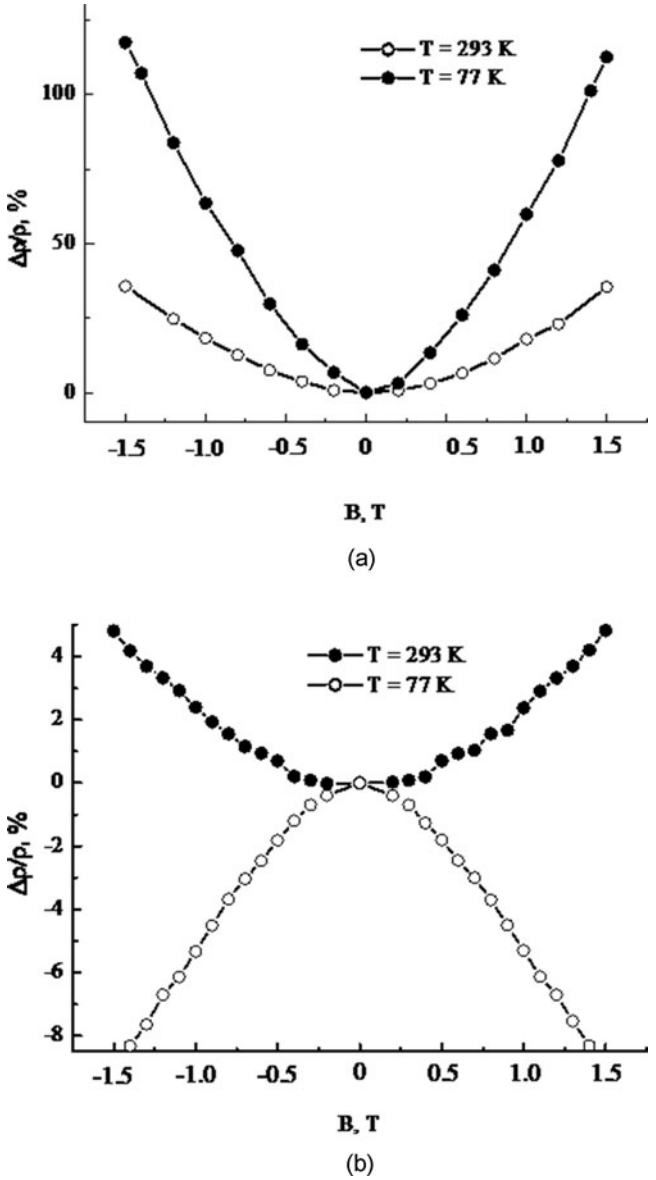

Figure 2. $\Delta\rho/\rho$(B) dependences for source HOPG (a) and FPG (b).

based on FPG, the temperature minima in the field dependences of the magnetoresistance are observed in all measurements.

Thus, the obtained experimental results allow us to state that a characteristic feature of the GICs with cobalt is the presence of the magnetoresistance asymmetric relative to the magnetic field direction.

As is already mentioned, there are no data on the graphite AMR in the literature, as well as the GICs with any other intercalates. However, the AMR effect was observed in layered structures containing incorporated magnetic metals. In particular, AMR was observed in multilayer films Co/Pd and Co/Pt [20], in epitaxial structures (Ga, Mn)/As [21], and in thin nickel films [22]. To explain the AMR in films with magnetic anisotropy, Segal et al. proposed a model [22], in which the anomalous dependence of the magnetoresistance on the magnetic

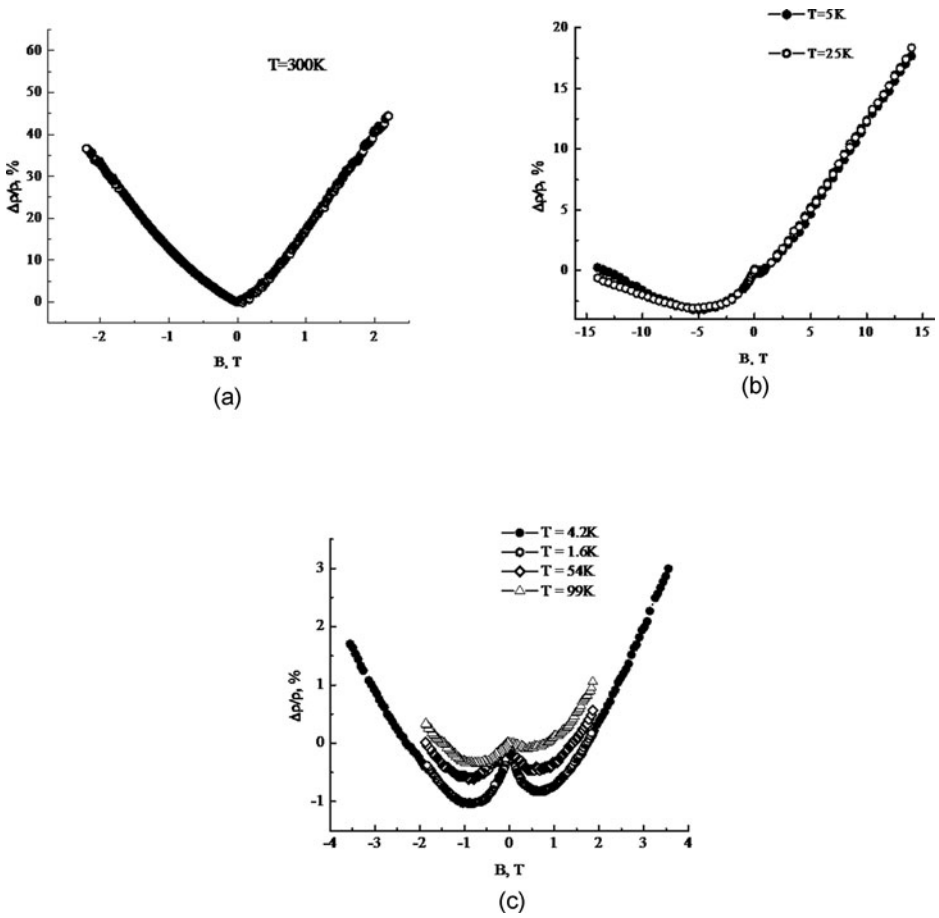

Figure 3. $\Delta\rho/\rho$ (B) dependences for GICs based on HOPG (a) and FPG, S = 2 (b) and S = 3 (c).

field direction is due to gradual variations in the magnetization and the Hall resistivity along the specimen. For the explanation of the AMR effect, Segal proposed to consider the specimen, in which the effect is observed, as a simple electric circuit (Fig. 4).

Here, $V_{AB}(H)$ and $V_{CD}(H)$ are transverse voltages in two different sections of the specimens. For magnetic materials, the transverse voltages generated due to the Hall effect are determined as

$$V_i = \frac{I}{t_i}\left(R_0 B + \mu_0 R_{EHEi} M_i\right), \tag{1}$$

where I is the electrical current, t_i is the thickness of specimens in a certain section (local thickness), R_0 and R_{EHEi} are, respectively, the ordinary and extraordinary Hall coefficients, and M is the magnetization. The resistances of AC and BD chains are equals ($R_{A\text{-}C} = R_{B\text{-}D} = R$) and according to Onsager's rule do not depend on the magnetic field direction. Following Kirchhoff's circuit laws, the longitudinal voltages at AC and BD chains are defined as

$$V_{AC} = \frac{IR + V_{AB} - V_{CD}}{2}, \tag{2}$$

$$V_{BD} = \frac{IR - V_{AB} + V_{CD}}{2}. \tag{3}$$

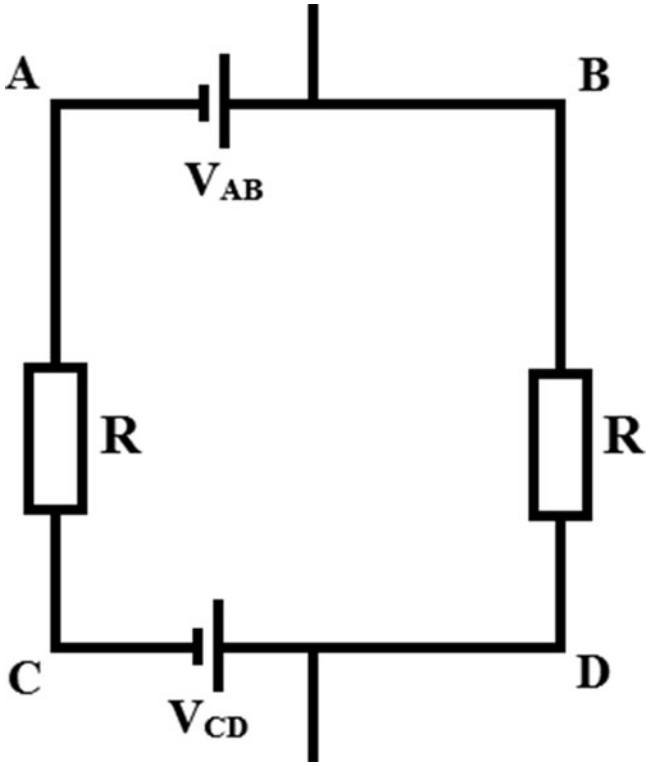

Figure 4. Effective electrical circuit presentation of GICs specimen [22].

As can be seen from these relations, the longitudinal voltages V_{AC} and V_{BD} aren't equal and differ from the ordinary Ohmic resistance 0.5IR, when the transverse voltages V_{AB} and V_{CD} aren't equal as well. Thus, the dependence of the longitudinal voltage and, consequently, the magnetoresistance on the magnetic field direction exists, if there is a heterogeneity of the transverse voltage distribution along a specimen. In this case, the voltage difference $V_{AB} - V_{CD}$ with the use of expression (1) can be written as

$$V_{AB} - V_{CD} = I\left(\frac{R_{0AB}B + \mu_0 R_{EHEAB}M_{AB}}{t_{AB}} - \frac{R_{0CD} + \mu_0 R_{EHECD}M_{CD}}{t_{CD}}\right)$$
$$= V_{AB}\left(1 - \frac{(R_{0CD} + \mu_0 R_{EHECD}M_{CD})\, t_{AB}}{(R_{0AB}B + \mu_0 R_{EHEAB}M_{AB})\, t_{CD}}\right). \quad (4)$$

Here, t_{AB} and t_{CD} are local thicknesses, M_{AB} and M_{CD} are local magnetizations, R_{0AB}, R_{EHEAB} and R_{0CD}, R_{EHECD} are the local ordinary and extraordinary Hall coefficients of AB and CD sections, respectively. These longitudinal voltages can be presented as

$$V_{AC} = \frac{IR}{2} - \alpha V_{AB}, \quad V_{BD} = \frac{IR}{2} + \alpha V_{AB}, \quad (5)$$

where α is coefficient depending on the thickness of magnetic clusters, values of ordinary and extraordinary Hall coefficients, and magnetization along the specimen. As is shown in (5), the first term is an even function of the magnetic field, and the second term is odd and is proportional to the transverse Hall voltage. The detailed calculations within the framework of the above representations for macroscopic specimens based on a detailed analysis of the mechanisms of electrical potential changes along the infinite specimen with variable thickness and

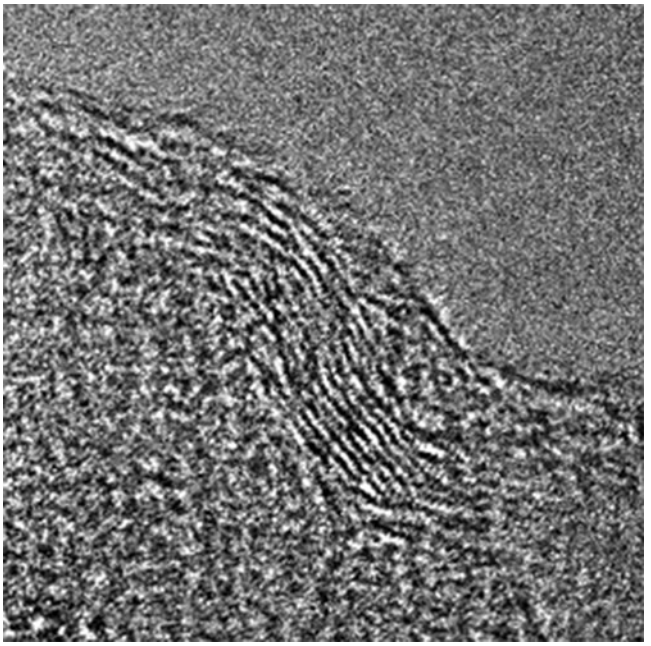

Figure 5. Fragment of electron microscopy image of GICs with cobalt [14].

Hall coefficient are presented in [22]. These calculations confirm the validity of assumptions (5).

Let us analyze the results of investigations of the magnetoresistance of GICs with cobalt in terms of the Segal model of asymmetric magnetoresistance. First, we consider the general characteristics of GICs with cobalt, which meet the requirements of the Segal model.

1. *Cluster structure of GICs with cobalt*. The electron microscopy studies of the structure [14] showed that GICs with cobalt are heterogeneous systems consisting of the graphite matrix, in which the clusters of intercalated graphite are distributed (Fig 5).

   There is a significant crushing of the graphite matrix during the intercalation process. The size of nonintercalated graphite parts is from 5 nm up to 20 nm. Nanoparticles of GICs with cobalt are situated in a graphite matrix quite uniformly, although they vary considerably in thickness. The size of intercalated graphite parts is in interval from 2 to 20 nm. Furthermore, the electron microscopy studies revealed that cobalt atoms are situated between the graphite layers. Thus, GICs with cobalt have a strongly heterogeneous structure. Compounds are composed of clusters of GICs and graphite clusters, and the sizes of all those clusters are variable along GICs specimens.
2. *Heterogeneity of magnetization*. As the studies of magnetic properties have shown, GICs with cobalt are layered ferromagnetic systems with high magnetic anisotropy [14]. The value of magnetization along the graphite plane (along the specimen) is almost an order of magnitude smaller than that along the C axis. A detailed study of the hysteresis loops of GICs with cobalt confirms the fact that these specimens are composed primarily of two-dimensional clusters of GICs, in which the ions of cobalt probably exhibit the antiferromagnetic or superantiferromagetic structure.
3. *Extraordinary Hall effect*. As was shown in [13], the formation of ferromagnetic (or antiferromagnetic) clusters of GICs in the graphite matrix leads to the appearance of the extraordinary Hall effect in these compounds caused by the spin-orbit interaction

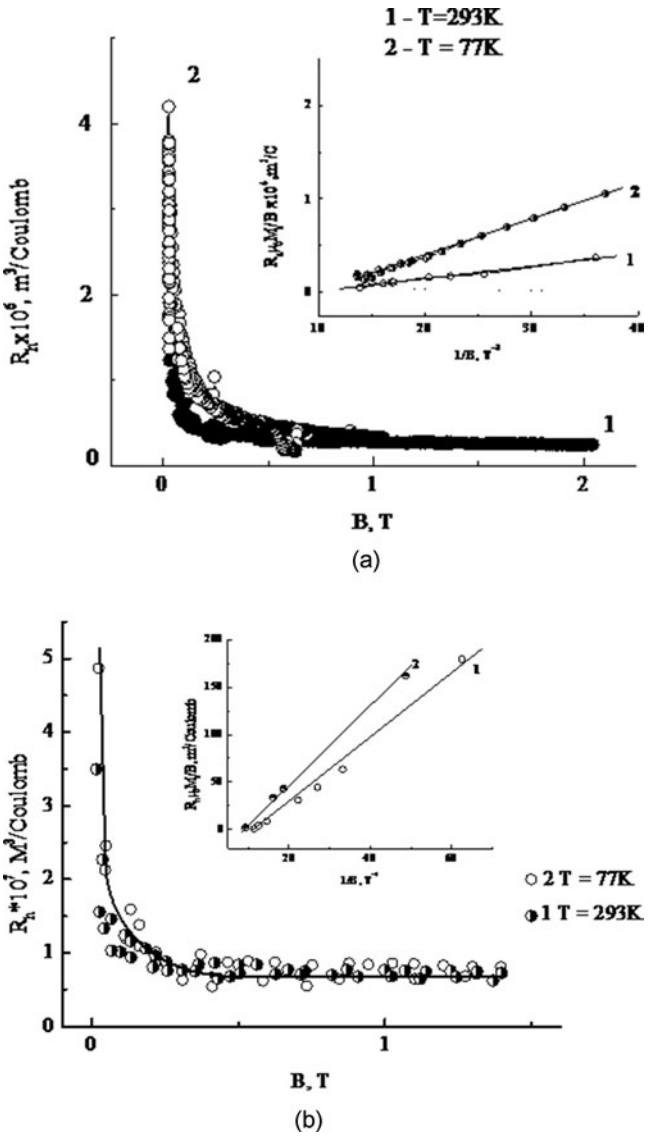

Figure 6. R_H(B) dependences for GICs with cobalt based on HOPG (a) and FPG (b); inset: dependences $R_A\mu_0 M/B$(1/B).

between the conduction electrons and carriers in the intercalate layer. Figure 6 presents the field dependences of the Hall coefficient for GICs with cobalt at room temperature and the temperature of liquid nitrogen.

As is seen from Fig. 6, there are two intervals in the dependence $R_H(B)$ at room temperature and $T = 77$ K: the interval of a drastic reduction of the Hall coefficient with increasing the magnetic field, and the interval, in which the Hall coefficient does not depend on the magnetic field. Given the structure of the compounds under study, namely, a high concentration of charge carriers in the layers of graphite, on the one hand, and the presence of magnetic clusters of GICs, on the other hand, it is appropriate to assume that the "asymmetric scattering," which includes the spin-orbit interaction between conduction electrons and magnetic moments of cobalt atoms, leads to the formation of the extraordinary Hall effect.

Thus, the GICs with cobalt are magnetic systems that are characterized by a high degree of heterogeneity. Such heterogeneity results in the inhomogeneous character of the magnetization and the Hall voltage along the specimens of GICs. These preconditions are the basis for the Segal model explaining the effect of AMR in specimens of GICs with cobalt.

Let us consider the magnetoresistance of GICs with cobalt in terms of the Segal model for AMR. According to (5), the electrical resistivity as a function of the magnetic field direction can be presented as

$$\rho\,(B) = \rho_e\,(B) + \rho_n\,(B)\,, \tag{6}$$

where $\rho_e(B)$ and $\rho_n(B)$ are the magnetoresistances even and odd relative to the magnetic field direction, respectively. The second term in (6) arises in the presence of a transverse voltage due to the variations of the size of magnetic clusters and the value of local Hall coefficient along the specimen. This term can be presented as $\rho_n(B) = \alpha B$, where α is some coefficient. Thus relation (6) can be rewritten as

$$\rho\,(B) = \rho_e\,(B) + \alpha B. \tag{7}$$

Figures 7 and 8a present the calculated dependences $\frac{\rho(\pm B)_{exper}}{\rho_0} \mp \beta B = f(\mp B),\ \beta = \frac{\alpha}{\rho_0}$, where ρ_0 is the resistivity without magnetic field for GICs based on HOPG (Fig. 7) and FPG (Fig. 8a) with cobalt.

As is seen from the above figures, the magnetoresistance symmetric relative to the magnetic field direction is observed for all specimens of GICs. Thus, the account for a magnetoresistance component linear in the magnetic field completely removes the asymmetry of the magnetoresistance for specimens of GICs with cobalt regardless of the type of a graphite source, stage of compounds, and temperature.

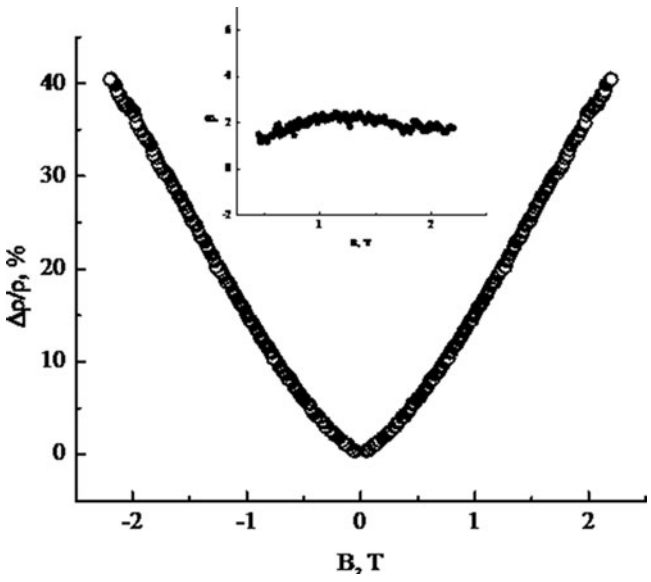

Figure 7. Dependence $\frac{\rho(\pm B)_{exper}}{\rho_0} \mp \beta B = f(\mp B)$ for GICs based on HOPG; inset: $\beta(B)$.

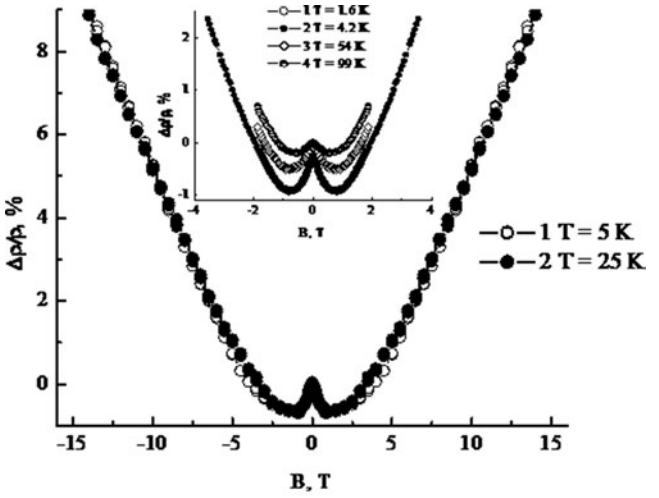

(a)

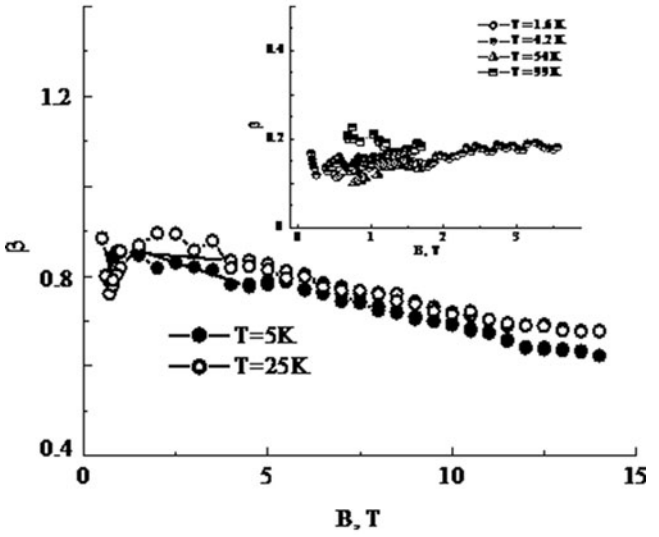

(b)

Figure 8. Dependences $\frac{\rho(\pm B)_{exper}}{\rho_0} \mp \beta B = f(\mp B)$ for second stage GIC based on FPG; inset: for third stage compound (a); dependence $\beta(B)$ for second stage GIC; inset: for third stage GIC (b).

The calculated dependences of the coefficient β on the magnetic field and temperature for GICs based on graphite with different structural perfections are shown in Figs. 7 (inset) and 8b.

As seen from the above figures, the very weak dependence of β on the magnetic field and temperature is observed for all GICs specimens. However, according to the figures, there is a significant dependence of the coefficient β on the structure of a source for the intercalation of graphite and on the number of stage. The greatest value of β is observed for GICs based on HOPG, $\beta \sim 2$. For the specimens of GICs based on FPG, the values of β are lower: for the second stage, β is $\sim$(0.7–0.8), and, for the third stage, β is $\sim$ (0.15–0.20).

According to (4) and (7), the coefficient β depends in a complicated manner on several parameters such as the values of ordinary and extraordinary Hall coefficients and magnetization in different sections of a GICs specimen and on the size of magnetic clusters (GICs clusters) in the specimen, as well as on the resistivity of GIC in zero magnetic fields. It is known [15] that, for low-stage compounds, the ordinary Hall coefficient is independent of the temperature and the magnetic field, which is confirmed by Fig. 6 (large magnetic field). As for the extraordinary Hall coefficient, then, as shown in Fig. 6 (inserts) for all investigated GICs, the value of $R_{EHE}\mu_0 M/B$ linearly depends on the temperature and slightly increases, as the temperature decreases. As was shown in [24], under the condition of "asymmetric scattering" of charge carriers, the following expression for the extraordinary Hall coefficient is correct:

$$R_{EHE} = a\rho + b\rho^2. \tag{8}$$

Here, ρ is the electrical resistivity, a and b are some coefficients. Thus, the temperature dependence of $R_{EHE}\mu_0 M/B$ is completely determined by the temperature dependence of the magnetization and, as follows from (8), the resistivity. Our results indicate that the temperature dependences of the resistivity for specimens of GICs based on HOPG and FPG are very weak (Fig. 9).

The temperature dependences of the magnetization along the graphite planes M_a for GICs with cobalt [14] have shown that the value of M_a in the small fields slightly increases, as the temperature decreases from 295 to 70 K.

Thus, according to experimental data [13, 14], the coefficient β for GICs with cobalt is really very weakly depends on the temperature and the magnetic field.

The larger value of β for the second-stage GICs based on FPG in comparison with the values of β for the third-stage compound is caused primarily to the fact that the production of low-stage specimens requires more "hard" conditions (high temperature, increase of the synthesis time). These conditions result in the formation of a highly defective structure of GICs. It is logical to assume, for lower-stage compounds, the reducing of the thickness of graphite clusters and GICs clusters and their substantial heterogeneity in thickness. This, as is seen from formula (4), is the main reason for the growth of the coefficient β.

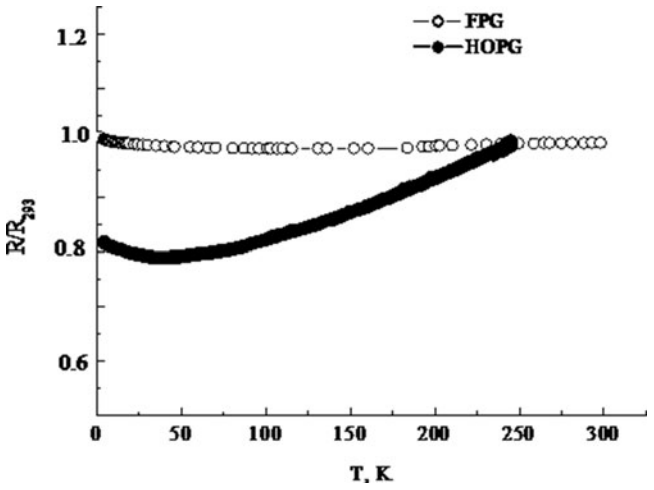

Figure 9. *$R/R_{293}(T)$* dependences for GICs with cobalt based on HOPG (1) and FPG (2).

Conclusion

The effect of the magnetoresistance asymmetric relative to a magnetic field was experimentally revealed in GICs with cobalt based on structurally perfect HOPG and on weakly ordered FPG. It had been experimentally proved that the value of AMR effect essentially depends on the structure of a source for the intercalation of graphite and on the stage of GICs. It is shown that this effect can be satisfactorily explained within the Segal model of asymmetric magnetoresistance in thin films with large magnetic anisotropy. It is established that the AMR effect is associated with a substantive heterogeneity of the GICs structure, namely, the presence of the magnetic clusters of GICs of different sizes in a graphite matrix. This leads, in turn, to a significant heterogeneity of the magnetization and variations in the Hall voltage of GICs specimens. Such phenomena are the preconditions of the occurrence of the AMR effect in GICs with cobalt. Within the Segal model, the resistance in a magnetic field can be considered as the sum of components, which are even and odd relative to the magnetic field. The account for the magnetoresistance component, which is odd relative to the magnetic field, completely removes the asymmetry of the magnetoresistance relative to the direction of the magnetic field.

References

[1] Mao, Y., Yuan, J., & Zhong, J. (2008). *J. Phys.: Condens. Matter.*, *20*, 115209.
[2] Fürst, Joachim A., Brandbyge, Mads, Jauho, Antti-Pekka, & Stokbro, Kurt. (2008). *Phys. Rev. B*, *78*, 195405.
[3] Ivanovskaya, V. V., Köhler, C.F., & Seifert, G. (2007). *Phys. Rev. B*, *75*, 075410.
[4] Karpan, V. M., Khomyakov, P. A., Starikov, A. A., Giovannetti, G., Zwierzycki, M., Talanana, M., Brocks, G., Brink, J., & Kelly, P. J. (2008). *Phys. Rev .B*, *78*, 195419.
[5] Yang, Chih-Kai, Zhao, Jijun, & Lu, Jian Ping. (2004). *Nano Lett.*, *4*, 561.
[6] Xiaojie, Liu, Wang, C. Z., Yao, Y. X., Lu, W. C., Hupalo, M. C., Tringides, M. C., & Ho, K. M. (2011). *Phys. Rev. B*, *83*, 235411.
[7] Krasheninnikov, A. V., & Nieminen, R. M. (2011). *Theor. Chem. Acc.*, *129*, 625.
[8] Hu, F. M., Tianxing Ma, Hai-Qing Lin, & Gubernatis, J. E. (2011). *Phys. Rev. B*, *84*, 075414.
[9] Ovsienko, I., Len, T., Matzuy, L., Prylutskyy, Yu., Berkutov, I., Andrievskii, V., Mirzoiev, I., Komnik, Yu., Grechnev, G., Kolesnichenko, Yu., Hayn, R., & Scharff, P. (2015). *Phys. Stat. Sol. (B)*, *252*, 1402.
[10] Ovsienko, I., Len, T., Matzuy, L., Tkachuk, V., Berkutov, I., Mirzoiev, I., Prylutskyy, Yu., Tsierkezos, N., & Ritter, U., (2016). *Mat.-wiss. u.Werkstofftech*, *47*, 254.
[11] Ovsienko, I. V., Matzui, L. Y., Yatsenko, I. V., Khrapatiy, S. V., Prylutskyy, Yu. I., Ritter, U., Scharff, P., & Normand, F. Le (2013). *Mat.-wiss. u.Werkstofftech*, *44*, 161.
[12] Len, T., Ovsienko, I., Matzuy, L., & Tkachuk, V. (2015). *J. of Nano- and Electronic Physics*, *7*, 02010–1.
[13] Matsui, D. V., Prylutskyy, Yu.I., Matzuy, L. Yu., Normand, F. Le, Ritter, U., & Scharff, P. (2008). *Physica E*, *40*, 2630.
[14] Matsui, D., Prylutskyy, Yu., Matzui, L., Zakharenko, N., Normand, F. Le, & Derory, A. (2010). *Phys. Stat. Sol. C*, *7*, 1264.
[15] Matsuy, D., Ovsienko, I., Lazarenko, O., Prylutskyy, Yu., & Matzui, V. (2011). *Mol. Cryst. and Liq. Cryst.*, *535*, 64.
[16] Matsuy, D., Ovsienko, I., Matzui, L., Prylutskyy, Yu., & Kunitskai, L. (2007). *Metallofiz. Noveish. Tekhn.*, *29*, 999.
[17] Xiang, G., & Zhang, X. (2011). *J. Phys.: Conf. Ser.*, *263*, 012013.
[18] Riss, O., Tsukernik, A., Karpovski, M., & Gerber, A. (2006). *J. Magn. Mater. 298*, 73.
[19] Gorbatsevich, A. A., Copaev, V. V., Copaev, Y. V., Kucherenko, A. V., & Omel'yanovskii, O. E. (2001). *Zh. Eksp. Teor. Fiz.*, *120*, 954.

[20] Cheng, X. M., Urazhdin, S., Tchernyshyov, O., Chien, C. L., Nikitenko, V. I., Shapiro, A. J., & Shull, R. D. (2004). *Phys. Rev. Lett.*, *94*, 017203.
[21] Xiang, G., Holleitner, A. W., Sheu, B. L., Mendoza, F. M., Maksimov, O., Stone, M. B., Schiffer, P., Awschalom, D. D., & Samarth, N. (2005). *Phys. Rev. B*, *71*, 241307R.
[22] Segal, O., Shaya, O., Karpovski, M., & Gerber, A. (2009). *Phys. Rev. B*, *79*, 144434.
[23] Matsuy, L. Yu., & Kotsyuba, A. M. (1999). *Visn. Kyiv Univ. Ser. Fiz. Mat. Nauk.*, *1*, 342.
[24] Granovsky, A. B., Kolitsov, A., & Brayers, F. (1997). *JETP Letters*, *65*, 509.